

Study on the effect of electron beam curing on low-K porous organosilicate glass (OSG) material

T.C. Chang^{a,b,*}, T.M. Tsai^c, P.T. Liu^{d,e}, C.W. Chen^c, T.Y. Tseng^c

^aDepartment of Physics and Institute of Electro-Optical Engineering, National Sun Yat-Sen University, 70 Lien-hai Rd., Kaohsiung 804, Taiwan, R.O.C.

^bCenter for Nanoscience and Nanotechnology, National Sun Yat-Sen University, Kaohsiung, Taiwan, R.O.C.

^cInstitute of Electronics, National Chiao Tung University, Hsin-Chu, Taiwan, R.O.C.

^dNational Nano Device Laboratory, 1001-1 Ta-Hsueh Rd., Hsin-Chu 300, Taiwan, R.O.C.

^eDepartment of Photonics and Display Institute, National Chiao Tung University, Hsin-Chu, Taiwan, R.O.C.

Abstract

The effect of electron beam (e-beam) curing on an ultra low dielectric constant material, porous organosilicate glass (OSG) is investigated. In conventional IC integration processes, photoresist (P. R.) stripping with O₂ plasma and wet chemical stripper is an inevitable step. However, dielectric degradation often occurs when low-k dielectrics undergo the PR stripping processing. This limits the application of incorporating low-k material into semiconductor fabrication. In order to overcome the integration issue, e-beam direct curing process was proposed in this study. In this technology, the dielectric regions irradiated by e-beam will be cross-linked, forming the desired patterns. Meanwhile, the regions without e-beam illumination are dissolvable in a mingled solvent of 2.38 wt.% tetra-methyl ammonium hydroxide (TMAH) and methanol with the ratio of 1:8. In this work, the possible doses of e-beam exposed porous OSG are decided by Fourier transform infrared spectroscopy, n&k 1200 analyzer and electrical analyses. The experimental results expressed that the minimum dosage to cure porous OSG film is 6 $\mu\text{C}/\text{cm}^2$, which is similar to commercial e-beam resist. Additionally, a scanning electron microscope \pm S.E.M.) image of homemade pattern was made to estimate the process practicability.

© 2004 Elsevier B.V. All rights reserved.

Keywords: Porous organosilicate; Low-K; E-beam; Direct patterning

1. Introduction

It has become apparent that utilizing low dielectric constant (low-k) materials as interlayer dielectric (ILD) for multilevel interconnect can effectively reduce resistance-capacitance (RC) delay and power consumption [1–5]. According to the ITRS roadmap of 2001 [6], it is necessary to reduce the dielectric constant of the ILD layers below 2.4 as the device dimension shrinks into sub-100 nm nanoscale fields. In addition to employ lower polarizability materials to decrease dielectric constant of the ILD layers, introducing

nanoscale pores into the dielectrics is an effective approach to achieve ultra low-k demand [7–11]. Among various porous low-k materials, porous organosilicate glasses (OSGs) are promising candidates for ILD application [12,13]. For further improving the chip performance, it is also a trend to integrate low-k materials with copper wiring to form damascene structure in multilevel interconnect [14,15]. Besides, it is required to simplify the fabrication procedures for interconnect architecture, especially etch-stop-layer, photoresist stripping, dry-etching process for damascene interconnect structure. However, porous low-k materials have been reported to be easily degraded during photoresist stripping processes due to their large internal surfaces [16,17]. Direct curing of low-k dielectrics using electron-beam (e-beam) exposure to form specific pattern is one of the promising choices to reduce process steps and avoid the damage from photoresist stripping during Cu

* Corresponding author. Department of Physics and Institute of Electro-Optical Engineering, National Sun Yat-Sen University, 70 Lien-hai Rd., Kaohsiung 804, Taiwan, R.O.C. Tel.: +886 3 5726100x7710; fax: +886 3 5722715.

E-mail address: tchang@mail.phys.nsysu.edu.tw (T.C. Chang).

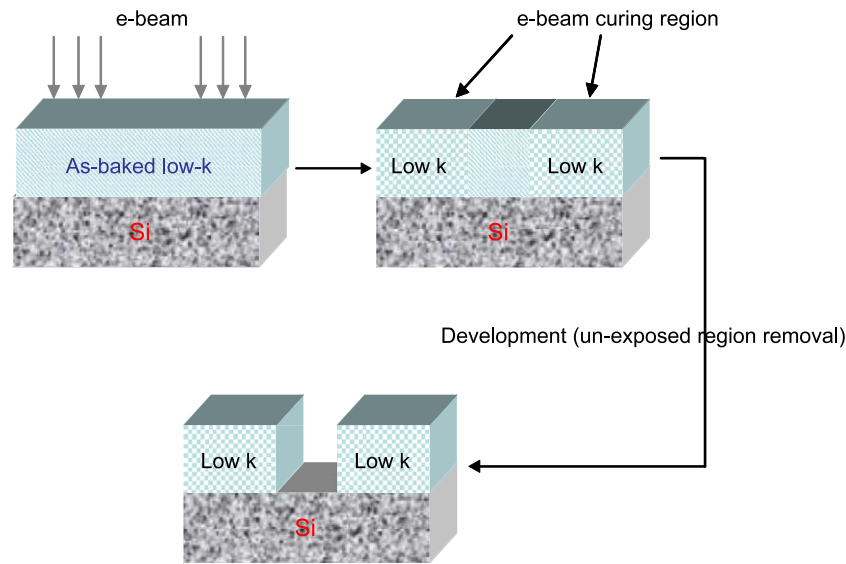


Fig. 1. Proposed e-beam direct curing process.

damascene manufacture. This process flow for forming single damascene pattern is shown in Fig. 1. Dual damascene structure also can be simply fabricated by twice porous OSG deposition/e-beam exposure processes for sequentially forming via and line patterns.

In this work, we investigate the effect of e-beam exposure on a porous OSG ($k=2.2$), which is manufactured by Chemat Technology and is based on a methyl-silsesquioxane matrix, except that it contains CH_n ($n=1-2$) bridging the siloxane networks ($-\text{Si}-\text{O}-\text{Si}-$). The material and the electrical analyses are performed to obtain the e-beam exposure dosage. Finally, the S.E.M. images will be observed to examine the practicability of using e-beam direct curing process.

2. Experimental

The substrates used in this study were 150 mm p-type (11–25 Ωcm) single crystal silicon wafers with (100) orientation. The precursor solution of the porous organosilicate glass (OSG) diluted with methylisobutylketone (MIBK) were spun on Si wafers at the first-stage spin rate of 450 rpm for 4 s and the second 3000 rpm for 30 s, respectively. As-spun wafers were baked at 100 $^\circ\text{C}$ on a hot plate for 1 min. The resulting wafers were exposed blankedly by a Leica Wepint200 e-beam stepper with doses ranging from 2 to 820 $\mu\text{C}/\text{cm}^2$. The e-beam energy was 40 KeV with beam size 20 nm. The exposure doses of e-beam irradiation could be determined according to material and electrical analyses. As for the pattern formation of porous OSG, as-baked samples were exposed with e-beam according to desire pattern layout. After e-beam irradiation, the resulted wafers were developed in a mixed solution containing 2.38 wt.% tetramethylammonium hydroxide (TMAH) and methanol with the ratio of 1: 8 and rinsed in deionized water until

the desirable pattern was completed. Furthermore, a furnace annealing process (at 400 $^\circ\text{C}$, 30 min) was performed on the e-beam exposed wafers to enhance dielectric properties of e-beam exposed porous OSG films. In addition, the control samples were also manufactured, according to a typical forming recipe, by transferring the as-spun wafers to a quartz furnace and heated from room temperature to 425 $^\circ\text{C}$ at a ramping rate of 20 $^\circ\text{C}/\text{min}$. After that, it is followed by thermal curing process at 425 $^\circ\text{C}$ for 1 h under nitrogen atmosphere. The refractive index and thickness of the above-mentioned porous OSGs were measured with an n&k analyzer. Infrared spectrometry was performed from 4000 to 400 cm^{-1} using a Fourier transform infrared (FTIR Bio-Red QS300) spectrometer calibrated to an unprocessed wafer for determining the chemical structures of all aforementioned samples. Electrical measurements were performed on metal insulator semiconductor (MIS) capacitors, which are constructed on e-beam exposed blanket porous OSG films through shadow mask. Dielectric constant measurements were conducted using a Keithley Model 82 CV analyzer. The area of gate electrode was 0.00503 cm^2 for C-V analysis. The leakage current (I-V) characteristics of dielectric were measured using a HP4156 electrical meter. Finally, the scanning electron microscope (\pm S.E.M.) image was conducted to examine the final pattern of e-beam cured porous OSG after development process.

3. Results and discussions

In order to determine the doses of e-beam curing on porous OSG film for direct patterning technology, a strategy based on material and electrical analyses should be proposed. Therefore, the effect of e-beam curing on the quality of porous OSG film through material and electrical analyses was investigated in this study. Fig. 2 shows the

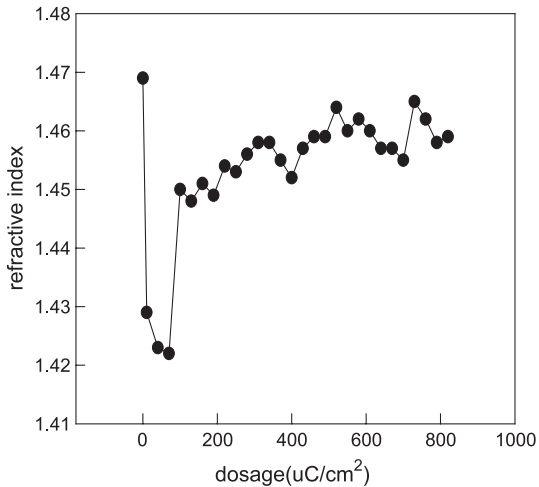


Fig. 2. The variation of refractive index of porous OSG films with electron beam exposed doses from 2 $\mu C/cm^2$ to 810 $\mu C/cm^2$.

refractive index varieties of porous OSG films with different e-beam exposed dosage from 2 to 810 $\mu C/cm^2$. The minimum refractive index is indicated from the figure to be present between 2 and 100 $\mu C/cm^2$. In addition, it is found that the region of porous OSG film without e-beam exposure cannot be removed entirely during the development process used in this study as the e-beam dosage exceed 100 $\mu C/cm^2$. This phenomenon is attributed to the proximity effect of e-beam exposure. Clearly, the findings revealed that the dosage of e-beam exposure cannot exceed 100 $\mu C/cm^2$. Fig. 3 reveals the remained thickness of the e-beam exposed porous OSG films with different dosage after development process. It was appeared that 70% thickness of the post-developed porous OSG films can be detained as the dosage exceeds 6 $\mu C/cm^2$. This implies that the threshold dosage of porous OSG material is about 6 $\mu C/cm^2$, which is similar to some commercial negative resist (e.g. SAL-601). As described above, the possible dosage range of e-beam curing on porous OSG films can be decided between 6 and

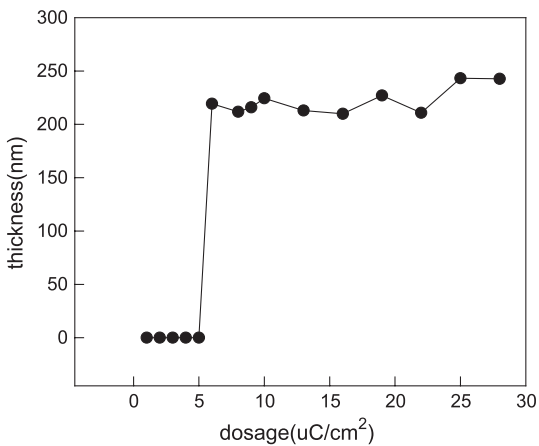


Fig. 3. The remained thickness of the porous OSG film after development with different dosage.

100 $\mu C/cm^2$. Therefore, the dielectric reactions between porous OSG films and e-beam exposure were first investigated to determine the optimized doses used on porous OSG films among the above dosage range. Fig. 4 shows the FTIR spectra of porous OSG films with different doses of e-beam exposure. In the furnace-cured porous OSG, Si–O stretching modes (cage-like at near 1144 cm^{-1} , network-like at near 1049 cm^{-1}), Si–C stretching peaks (at 781, 1273 cm^{-1}), and C–H peak (2980 cm^{-1}) are appeared in the FTIR spectra. After e-beam exposure, the peaks of Si–O stretching vibration significantly change. E-beam exposure provides the as-baked porous OSG film energy to be cross-linked and transfer the porous OSG film from cage-like structure to network-like one. It clearly reveals the intensity of Si–O network mode grows at the expense of the intensity of Si–O cage-like mode with increasing e-beam exposure doses. This indicates the structure of the porous OSG film changes from the cage-like to a stable three-dimensional network structure via the breakage of Si–O cage-like and subsequently forming Si–O–Si network.

The leakage current density and dielectric constant of e-beam exposed porous OSG films were also evaluated so as to satisfy the requirement of inter-metal dielectric applications. The leakage current densities of e-beam exposed at different doses were presented in Fig. 5. It is observed that the leakage current of all e-beam exposed porous OSG films is larger than that of furnace-cured one. Nevertheless, the leakage current of e-beam exposed porous OSG film with a dose of 10 $\mu C/cm^2$ has the lowest value. While the exposure dosage reaches 16 $\mu C/cm^2$, the leakage current of e-beam exposed porous OSG film will increase one order of magnitude than that of furnace-cured one at 1 MV/cm electric field. Fig. 6 shows the dielectric constant of e-beam exposed porous OSG films at different doses. The results indicate that the dielectric constant of e-beam exposed films

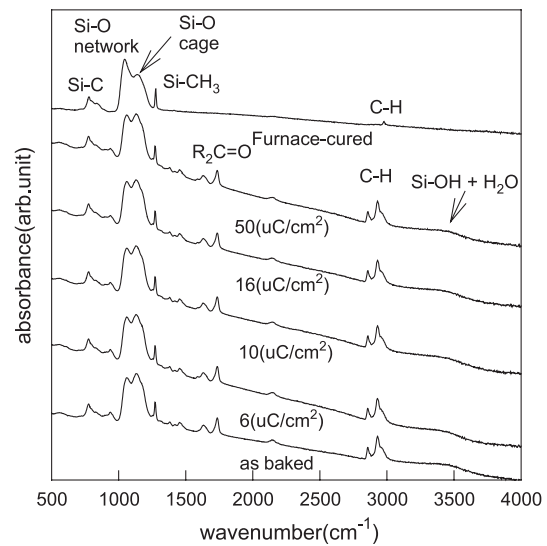


Fig. 4. FTIR spectra of porous OSG films with different doses of electron beam exposure.

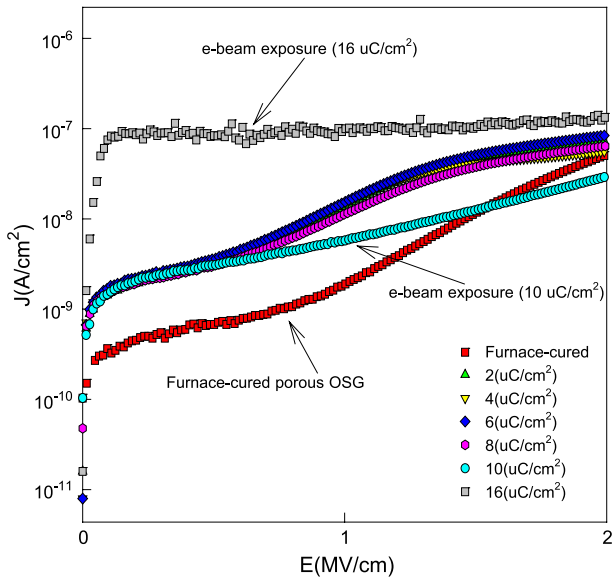


Fig. 5. The leakage current densities of e-beam exposed porous OSG films at different doses.

with all different doses is larger than that of furnace-cured one. According to aforementioned electrical analyses, the dielectric loss is inferred to be due to the formation of dangling bond owing to e-beam exposure and the adsorption of polarized components such as moisture in porous OSG films after the e-beam exposed dose over than 10 $\mu\text{C}/\text{cm}^2$. The inference can be demonstrated from the FTIR spectra in Fig. 4. The intensity of Si–OH and moisture bonds around 3400 cm^{-1} will increase as the dosage exceeds 10 $\mu\text{C}/\text{cm}^2$. This implies that the e-beam dosage cannot be too high to obtain the required dielectric properties of ultra low-k porous OSG. In this work, the optimum e-beam exposure dosage was obtained with a dose of 10 $\mu\text{C}/\text{cm}^2$. As a result

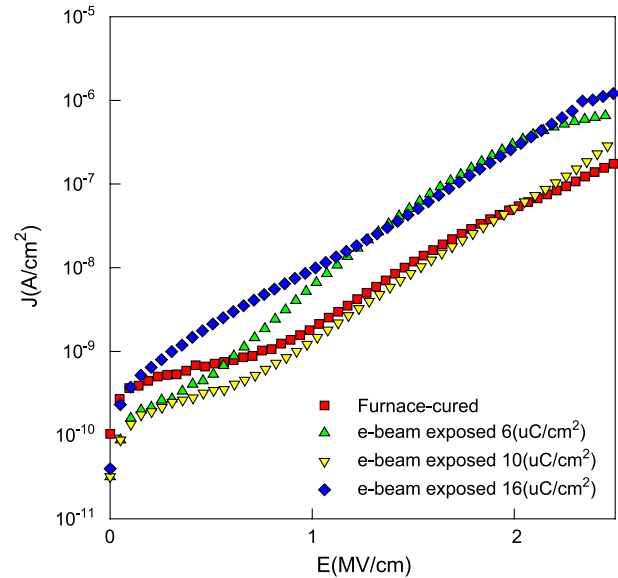


Fig. 7. The leakage current densities of e-beam exposed porous OSG films at different doses with furnace annealing process.

of the electrical properties of e-beam, exposed porous OSG films at different e-beam exposed doses are all inferior to that of standard furnace-cured ones, thus we tried transferring these wafers to a furnace for further thermal annealing. Fig. 7 reveals the leakage current densities of e-beam exposed porous OSG films at different doses with an additional annealing in a furnace at 400 °C for 30 min. It is clear that the leakage current densities are all significantly reduced after thermal annealing. Especially for the e-beam-exposed sample with the dose of 10 $\mu\text{C}/\text{cm}^2$, its' leakage current density is recovered close to that of the furnace-cured one. The dielectric constant of e-beam exposed porous OSG films at different doses with thermal annealing is also

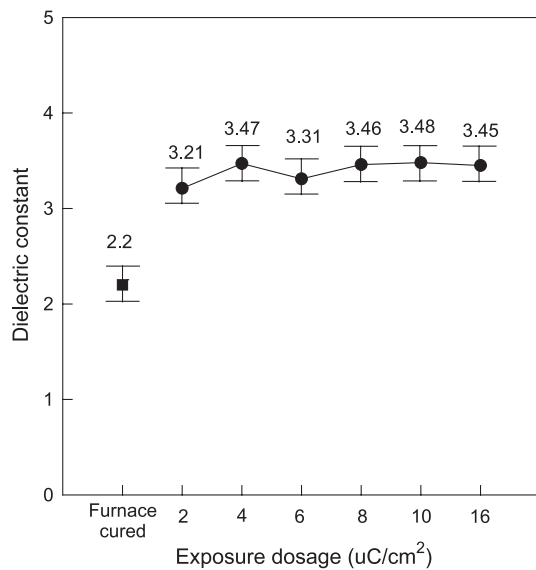


Fig. 6. Dielectric constant of e-beam exposed porous OSG films at different doses.

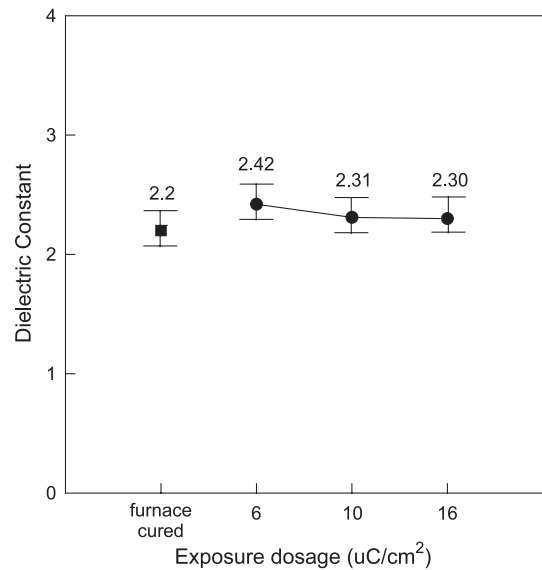


Fig. 8. The dielectric constant of e-beam exposed porous OSG films at different doses with furnace annealing process.

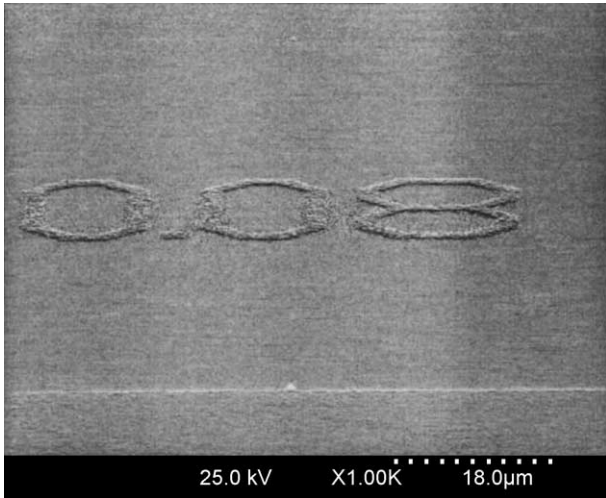


Fig. 9. The S.E.M. image of patterned wafer after e-beam curing and development processes without post-exposure annealing.

shown in Fig. 8. It is demonstrated that the dielectric constants of porous OSG films after e-beam exposure with thermal annealing in a furnace are decreased and close to the standard furnace-cured one. This indicates that even though the dielectric constants of porous OSG films after e-beam exposure are higher than that of the furnace-cured one, it can be recovered by additional thermal annealing process. Therefore, the results suggest that though available electrical dielectric properties of porous OSG film cannot be obtained directly by the e-beam curing process, the post-exposed thermal annealing process can be utilized to recover the electrical dielectric characteristics as the desirable pattern is formed by e-beam direct patterning process.

Finally, a homemade pattern was formed by e-beam direct patterning to estimate its practicability. In this study, we used a mixed solution containing 2.38 wt.% tetramethylammonium hydroxide (TMAH) and methanol with the ratio of 1: 8 to develop the pattern, and the result is shown in Fig. 9. Although the well contract of the pattern was not observed after development, it is clear that the e-beam direct patterning process can be achieved on porous OSG films. An additional study is required to perfect the patterning resolution, but it is believed that this can be fine-tuned by varying the e-beam exposure dose and developed time.

4. Conclusions

The e-beam direct curing process for low-k porous OSG as inter-metal dielectric (IMD) has been investigated in this paper. The novel direct patterning technology on the porous OSG can avoid the damage during conventional photoresist removal process. The material analysis shows that the e-beam curing can effectively provide porous OSG films energy to make the cage-like bonds of porous OSG transfer to network bonds. Then, the part of porous OSG films

without e-beam cured can be developed using the mixed solvent of 2.38 wt.% tetra-methyl ammonium hydroxide (TMAH) and methanol. In addition, the leakage current density and dielectric constant of e-beam exposed porous OSG films can be recovered by post-exposure thermal annealing in a furnace.

Acknowledgment

This work was performed at National Nano Device Laboratory, Taiwan, ROC and was supported by National Science Council of the Republic of China under contrast No. NSC 92-2215-E-009-020 and NSC NSC92-2112-M-110-020. The authors also gratefully acknowledge the support from Dr. Jay C-J. Chu and Chemat Technology Inc., USA.

References

- [1] G. Sugahara, N. Aoi, M. Kubo, K. Arai, K. Sawada, International Dielectrics for ULSI Multilevel Interconnection, Proceedings of the Conference, 1997, p. 19.
- [2] P.T. Liu, T.C. Chang, S.M. Sze, F.M. Pan, Y.J. Mei, W.F. Wu, M.S. Tsai, B.T. Dai, C.Y. Chang, F.Y. Shin, H.D. Hung, Thin Solid Films 332 (1998) 345.
- [3] P.A. Kohl, Q. Zhao, K. Patel, D. Schmidt, S.A. Bidstrup-Allen, R. Shick, S. Jayaraman, The Electrochemical Society Proceedings in Dielectric Materials Integration for Microelectronics, Series, Pennington, NJ, 1998, p. 169.
- [4] P.T. Liu, T.C. Chang, Y.L. Yang, Y.F. Cheng, S.M. Sze, IEEE Trans. Electron Devices 47 (2000) 1733.
- [5] J. Taniguchi, K. Kanda, S. Matsui, M. Tokunaga, I. Miyamoto, 2001 International Microprocesses and Nanotechnology Conference, Tokyo, Japan, 2001, p. 208.
- [6] The National Technology Roadmap for Semiconductors, Semiconductor Industry Association, San Jose, CA, 2001.
- [7] N.P. Hacker, Mater. Res. Bull. 22 (1997) 33.
- [8] R.J. Gutmann, W.N. Gill, T.M. Lu, J.F. McDonald, S.P. Murarka, E.J. Rymaszewski, Advanced Metallization Conference in 1996, Materials Research Society, Pittsburgh, PA, 1997.
- [9] E.T. Ryan, A.J. McKerrow, J. Leu, P.S. Ho, Mater. Res. Bull. 22 (1997) 49.
- [10] M.R. Baklanov, E. Kondoh, E.K. Lin, D.W. Gidley, H.J. Lee, K.P. Mogilnikov, J.N. Sun, Proceedings of IITC'2001, San Francisco, CA, 2001, p. 189.
- [11] F. Schueth, W. Schmidt, Adv. Mater. 14 (2002) 629.
- [12] P.A. Kohl, A. Padovani, M. Wedlake, D. Bhusari, S.A. Bidstrup-Allen, R. Shick, L. Rhodes, Mater. Res. Soc. Symp. Proc. 565 (1999) 55.
- [13] J. Liu, D. Gan, C. Hu, M. Kiene, P.S. Ho, W. Volksen, R.D. Miller, Appl. Phys. Lett. 81 (2002) 4180.
- [14] D. Louis, C. Arvet, E. Lajoinie, C. Peyne, S. Lee, I. Berry, Q. Han, Microelectron. Eng. 53 (2000) 381.
- [15] J.P. Reynard, C. Verove, E. Sabouret, P. Motte, B. Descouts, C. Chaton, J. Michailos, K. Barla, Microelectron. Eng. 60 (2002) 113.
- [16] P.T. Liu, T.C. Chang, Y.S. Mor, C.W. Chen, T.M. Tsai, C.J. Chu., F.M. Pan, S.M. Sze, Electrochem. Solid-State Lett. 5 (2002) G11.
- [17] Y.S. Mor, T.C. Chang, P.T. Liu, T.M. Tsai, C.W. Chen, S.T. Yan, C.J. Chu, W.F. Wu, F.M. Pan, W. Lur, S.M. Sze, J. Vac. Sci. Technol. B 20 (2002) 1334.